JOURNAL GEOLOGICAL SOCIETY OF INDIA
Vol.94, July 2019, pp.62-68

Geology-aided Geostatistical Modelling of a Ferruginous Bauxite Deposit in Eastern India

Girija Shankar Behera, Bhabesh C. Sarkar*, Rahul Kumar Singh, Sahendra Singh
Department of Applied Geology, Indian Institute of Technology (Indian School of Mines), Dhanbad – 826 004, India
***E-mail:** bhabeshsarkar2005@gmail.com*

ABSTRACT

Geostatistical modelling for a part of a ferruginous bauxite deposit in Eastern India has been carried out for estimation of mineral inventory and grade-tonnage relationships. Resource estimation of the bauxite deposit carried out by different agencies previously were on the basis of drill hole spacing employing fundamentally conventional cross-sectional techniques and in a limited way geostatistics. The conventional methods have limitation to specify the confidence limits (+/-) or, in other words, the percent accuracy of the estimated mean. One normally relies on approximation without any mathematical basis. However, no integrated mineral deposit modelling has been carried out combining deposit geology with geostatistics for development of mineral inventory and estimation of grade-tonnage relationships. An understanding of formation of bauxite by the process of residual weathering and lateritization of Archean khondalite and charnokite, when incorporated in population modelling and semi-variography and integrated with appropriate geostatistical evaluation process provided a means to improved geo-characterization of the bauxite deposit. The integrated geostatistical modelling led to the quantification of the individual population characteristics and spatial relationships of the geo-variables. Spatial correlation modelling of the sample values through semi-variography revealed a moderate to high nugget-to-sill ratio with moderate range of influence, characterizing the spatial variability of the ferruginous bauxite deposit. Geostatistical estimation employing 3D block kriging led to the generation of slice-wise block kriged estimates and kriging variances. Resulting block estimates, when stacked slice-wise one below the other, provided a 3D mineral inventory of 29.87 mt of bauxite averaging 42.04% Al_2O_3 and 2.88% SiO_2. Spatial distribution maps of kriging variance aid in reflecting zones of uncertainty of varying magnitude associated with block estimates.

INTRODUCTION

Bauxite deposit studied for geostatistical modelling is one of the largest known bauxite deposits in India. The deposit is located between latitudes 18°48'N and 18°54'N; longitudes 82°57'E and 83°04'E and falls in the survey of India topographic map numbers 65 J/13 and partly in 65 N/1. The bauxite occurs on plateau top as blanket deposit. The plateau elongates over a length of about 21 km trending NE-SW with width varying from 1.8 km to as low as 100 m. The plateau is generally flat on top with average elevation 1350 m above mean sea level, rising by about 150 m to 300 m above the adjoining plains and valleys. Different ore types associated with the deposit are mainly gibbsite, hematite and goethite. Depositional process of bauxite formation being residual concentration, it is important to understand lateral and vertical relationships of constituent variables for 3D spatial variability modelling of the bauxite deposit. The approach combines an understanding of the deposit geology (Sarkar, 2014a, b) with classical statistics and geostatistics for estimation of mineral inventory and grade-tonnage relationships (Saikia and Sarkar, 2013). The integrated geostatistical modelling study is aimed at delivering an objective means to geo-characterization of the bauxite deposit and to obtain improved estimates.

GEOLOGY

The bauxite deposit under study is a flat-topped hill with five wide-ranging and short peaks and belongs to the Eastern Ghats mobile belt (EGMB) (Sen and Guha, 1987a; Sharma, 2009; Ramakrishnan and Vaidyanadhan, 2010). A geological map of the deposit is shown in Fig.1 (after Subrahmanyam et al., 1996). Dominant rock assemblage in the area comprises of khondalite and charnockites of Archaean age. Depositional process of the bauxite deposit is governed by weathering and residual concentration of khondalite and charnockites (Sengupta et al., 1991). A schematic litho-stratigraphic succession of the bauxite deposit is presented in Fig.2. The oxides other than A1, Fe and Ti have been almost completely removed from the bauxitic part of the weathering profile. Such differential leaching is favored by different Eh and pH conditions. $A1_2O_3$ and Fe_2O_3 emerge as the major constituents controlling the overall composition and grade of the bauxite ore (Sen and Guha, 1987b). The deposit is heterogeneous in

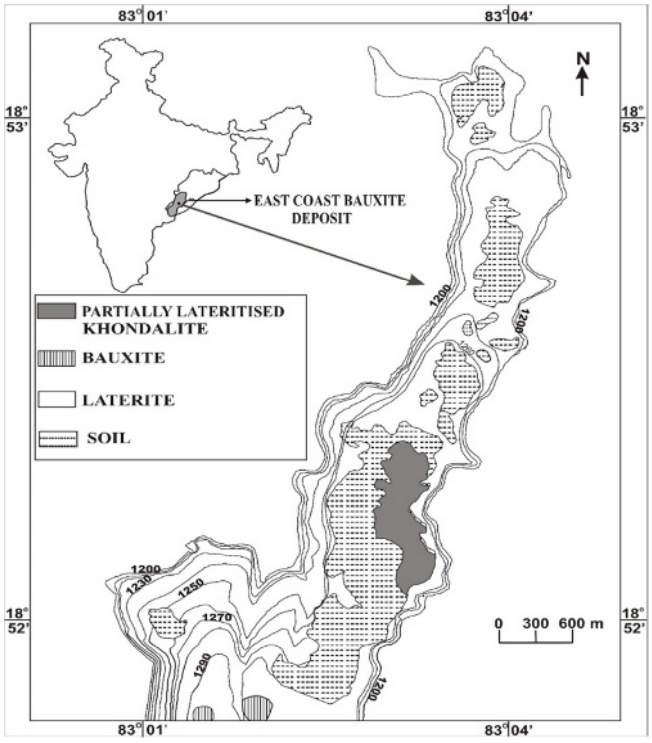

Fig.1. Geological map of the bauxite deposit (after Subrahmanyam et al. 1996).

DOI: 10.1007/s12594-019-1267-9 | 0016-7622/2019-94-1-62/$ 1.00 © GEOL. SOC. INDIA

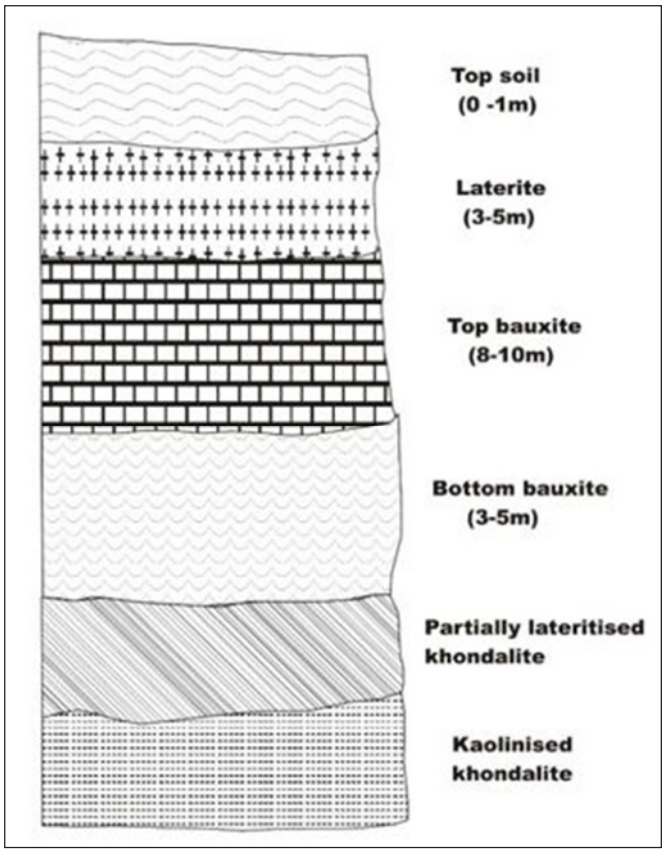

Fig. 2 A schematic litho-stratigraphic succession of the bauxite deposit

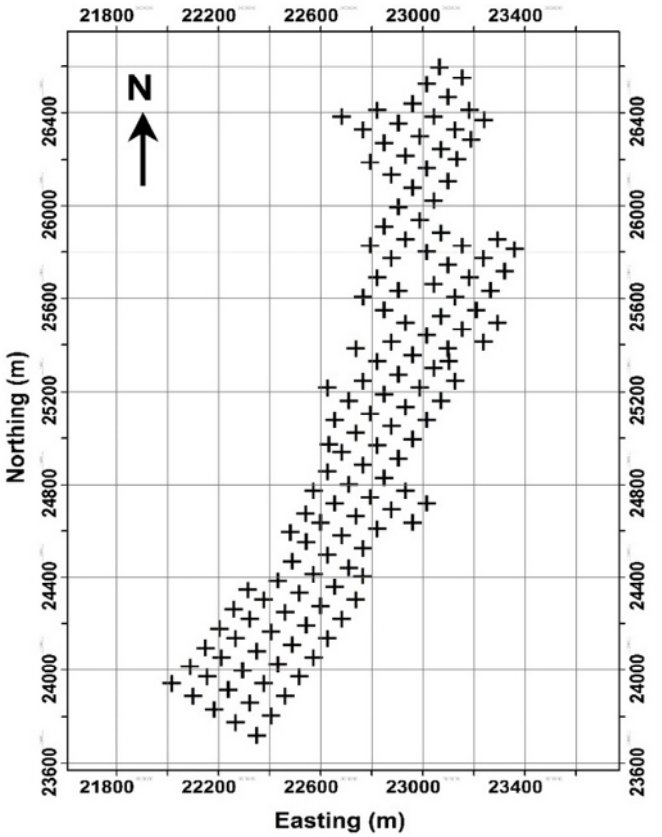

Fig. 3 Location plan of exploratory drill holes

terms of lateral and vertical variations in grade and thickness. An examination of the drill core assay values suggests that the vertical variation in grade and thickness is much more than the lateral variation. Transition zones between bauxite and laterite at the top and that between bauxite and partially lateralized khondalite at the bottom are highly undulated due to differential leaching process (Babu et al., 2014). The lateritic bauxite deposit is iron rich, which is one of the distinctive characteristics of the bauxite deposit, owing to its association with gibbsite, hematite and goethite ore types (Bhukte and Chaddha, 2014).

DATABASE AND METHODOLOGY

Drill hole assay data with 3D spatial coordinates pertaining to the north block of the deposit have been used in the present study for the integrated geostatistical modelling and mineral inventory estimation. A location plan of drill holes is displayed in Fig.3. A source database has been developed from unpublished exploration reports constituting available geological and exploration data of the bauxite deposit. In all, 3321 drill core samples, pertaining to 125 vertical drill holes with a lateral drill hole spacing of 50m to 100m, have been subjected to sample value. This led to 1017 number of sample value composites of 2m vertical length. The composite sample database consists of 3D spatial coordinates of the centroid of the vertical composite, viz. easting (X), northing (Y) and elevation (Z) corresponding to composite sample values of Al_2O_3 (≥ 20%), SiO_2 (≤ 7%), Fe_2O_3 and TiO_2. Exploratory data analysis (EDA) carried out through histogram analyses and probability plots did not reveal presence of any outlier(s). The composite sample database has then been used to carry out statistical and geostatistical analyses of the bauxite deposit.

A step-wise statistical and geostatistical techniques and tools employed for the integrated geostatistical modelling include (i) population modelling (Wellmer, 1998) using classical statistics to detect for mixed population, if any and to characterize the frequency distributions of Al_2O_3, SiO_2, Fe_2O_3 and TiO_2 geo-variables of the bauxite deposit; (ii) 3D experimental semi-variogram analyses of the variables to understand spatial variability and relationship among sample values; (iii) fitting of appropriate mathematical function to experimental semi-variograms to estimate nugget effect (C_o), continuity variance (C) and range of influence (a); (iv) selection of suitable block size based on criteria of average drill hole spacing, mining method, size of mining equipment and targeted production per day; (v) generation of vertical cross-sections and horizontal slice plans; (vi) work plan constituting delineation of mineralized boundaries as slice plans with respect to block-sized grid and specified blocks to be kriged; (vii) development of slice-wise block matrix; (viii) estimation of block values (kriged estimates) and associated error of estimation (kriging variance); (ix) estimation of bauxite mineral inventory by stacking slice-wise all kriged blocks; (x) estimation of grade-tonnage relationships involving a step-wise integration of the block grade frequency distribution over a range of block grades.

Population Modelling

Frequency distributions analysis of raw sample value composites in respect of Al_2O_3, SiO_2, Fe_2O_3 and TiO_2 revealed a skewed distribution. Probability model fit exercise revealed a single population for all the variables with a negatively skewed 3-parameter lognormal distribution for Al_2O_3, a positively skewed 3-parameter lognormal distribution for SiO_2, a negatively skewed 3-parameter lognormal distribution for Fe_2O_3 and a positively skewed 2-parameter lognormal distribution for TiO_2. Histograms and probability diagrams are displayed in Fig.4 and the summary statistics are provided in Table 1. Al_2O_3 being relatively less mobile than Fe_2O_3 and much less than SiO_2 and TiO_2, undergoes relative residual enrichment during process of lateritization. Bauxite profile displays very low concentration of SiO_2 (ranging between

Table 1. Summary statistics of geo-variables

Variables		Al_2O_3	SiO_2	Fe_2O_3	TiO_2
No. of samples		1017	1017	1017	1017
Minimum (%)		20.76	0.37	6.13	0.95
Maximum (%)		56.93	7.00	53.17	5.06
Mean (%)		41.78	2.81	27.28	2.07
Variance $(\%)^2$		23.97	3.43	41.73	0.21
Standard deviation (%)		4.89	1.85	6.46	0.46
Skewness		-0.25	0.70	-0.16	0.90
Kurtosis		3.70	2.28	3.12	5.99
χ^2 computed value		36.01	416.31	154.25	22.05
χ^2 table value(α=0.05)		14.07	19.68	12.59	7.81
		$\nu = 7$	$\nu = 11$	$\nu = 6$	$\nu = 3$
Statistics of log-transformed data					
Log mean (%)		5.2560	1.7123	3.6026	0.69
Log variance $(\%)^2$		0.0006	0.0932	0.0337	0.04
Log standard deviation (%)		0.0261	0.3053	0.1837	0.22
Log skewness		-0.33	0.35	-0.77	-0.02
Log kurtosis		3.52	1.87	3.97	3.39
Additive constant		150	3	10	0
Average		41.77	2.80	27.31	2.04
Central 90% Confidence limits	Lower limit(%)	41.57	2.71	26.98	2.02
	Upper limit(%)	41.96	2.90	27.51	2.07
Population distribution		Negatively skewed 3-parameter lognormal	Positively skewed 3-parameter lognormal	Negatively skewed 3-parameter lognormal	Positively skewed 2-parameter lognormal

0.37% and 7.00%). The mode of occurrence of SiO_2 in bauxite profile suggests a very fast leaching and removal of SiO_2 during bauxitisation process. It may be inferred that negatively skewed 2-parameter lognormal distribution of Al_2O_3 and a positively skewed 3-parameter lognormal distribution for SiO_2 is a significant reflection of the geological process of bauxite formation as evident in the deposit. The deposit being ferruginous contains Fe_2O_3 values in the range of 6.13% and 53.17% and is characterized by a negatively skewed 3-parameter lognormal distribution. The deposit contains a low TiO_2 in the range of 0.95% and 5.06% and thus exhibits a positively skewed distribution. The frequency distribution modelling study of the variables provided representative probability density function, f(x) expressed below as:

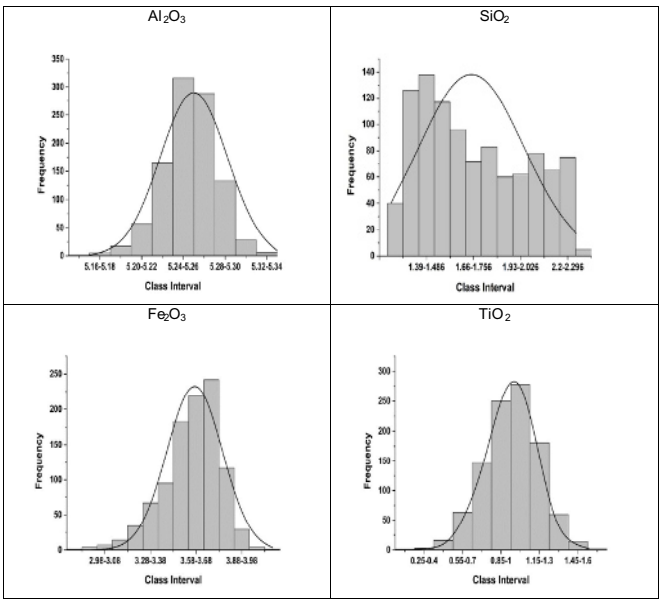

Fig.4 Histograms and probability plots of log-transformed geo-variables

$$f(x) = \frac{1}{x*0.0261\sqrt{2\pi}}\, e^{-0.5\left[\frac{\ln x - 5.256}{0.0261}\right]^2}, \text{ for } Al_2O_3 \quad (1)$$

$$f(x) = \frac{1}{x*0.3053\sqrt{2\pi}}\, e^{-0.5\left[\frac{\ln x - 1.7123}{0.3053}\right]^2}, \text{ for } SiO_2 \quad (2)$$

$$f(x) = \frac{1}{x*0.1837\sqrt{2\pi}}\, e^{-0.5\left[\frac{\ln x - 3.6026}{0.1837}\right]^2}, \text{ for } Fe_2O_3 \quad (3)$$

$$f(x) = \frac{1}{x*0.22\sqrt{2\pi}}\, e^{-0.5\left[\frac{\ln x - 0.69}{0.22}\right]^2}, \text{ for } TiO_2 \quad (4)$$

Semi-variography

Geostatistical analyses involving spatial correlation study of the geo-variables in the bauxite deposit has been carried out through semi-variography. To identify whether or not directional anisotropy exist, experimental semi-variograms were initially constructed along four principal directions, viz. 0°, 45°, 90° and 135° (Diko et al., 2001; Pyrcz and Deutsch, 2006) with a lag interval of 50m (for 0° and 90° directions), 70m (for 45° and 135° directions), an angle of regularization of 11.25° and a spread limit of two times the lag interval (Olea, 1999) for Al_2O_3, SiO_2, Fe_2O_3 and TiO_2 variables. Since the directional semi-variograms did not have adequate sample pairs, a 3D omni-directional semi-variogram was constructed for each of the variables with a lag distance of 50m. Suitable mathematical functions have then been fitted to the 3D omni-directional experimental semi-variograms employing Point Kriging Cross-Validation technique (Sarkar et al., 1988). This led to fit of a spherical mathematical scheme to the experimental semi-variograms. Graphical plots of experimental semi-variograms of the variables with fitted spherical models are shown in Fig.5 and the summary of semi-variogram analyses are given in Table 2. Behaviour of semi-variogram function near the origin provided an estimate of nugget effect with high degree of random (unexplained) component of semi-variance, which is characteristic of the bauxite deposit owing to residual concentration process of formation. The range of influence of the semi-variogram models varies from 170m to 260m depending upon the sample-to-sample influence for the individual variables. Spherical functions fitted to the experimental semi-variograms are numerically expressed in the following numerical relationships:

$$\gamma(h) = 15.75+8.05[(1.5) \times (50/170)-0.5\times (50/170)^3], \text{ for } Al_2O_3 \ldots\ldots\ldots (5)$$

$$\gamma(h) = 2.33+1.08\,[(1.5) \times (50/220)-0.5\times (50/220)^3], \text{ for } SiO_2 \ldots\ldots\ldots (6)$$

$$\gamma(h) = 31+10.73[(1.5) \times (50/260)-0.5 \times (50/260)^3], \text{ for } Fe_2O_3 \ldots\ldots\ldots (7)$$

$$\gamma(h) = 0.153+0.056\,[(1.5) \times (50/170)-0.5\times (50/170)^3], \text{ for } TiO_2 \ldots\ldots\ldots (8)$$

The semi-variography revealed a nugget-to-sill ratio of 0.66 for Al_2O_3, 0.68 for SiO_2, 0.74 for Fe_2O_3 and 0.73 for TiO_2 respectively. A moderate to high nugget-to-sill ratio with moderate range of influence, as revealed from the respective fitted spherical semi-

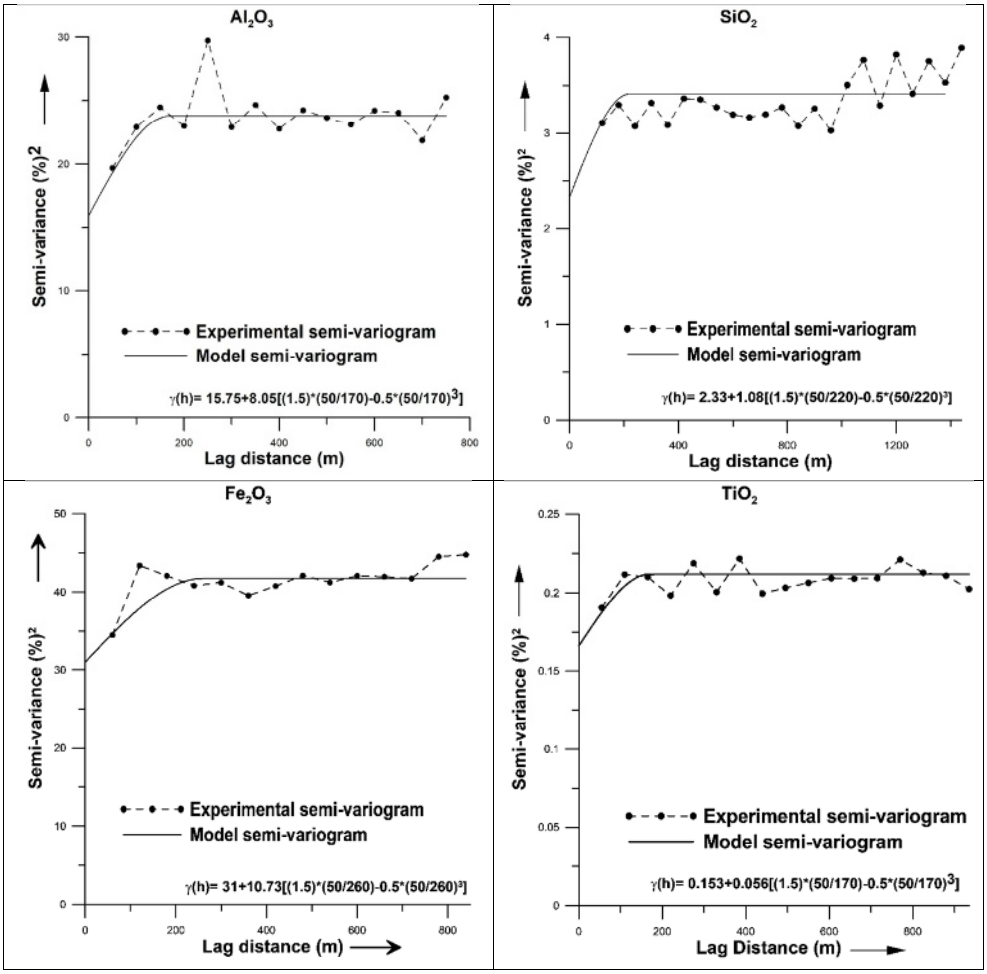

Fig.5. Experimental semi-variograms with fitted models of constituent geo-variables

variogram functions, is a geostatistical characteristic reflecting bauxite deposit formed due to the weathering and residual concentration process.

Table 2 Summary of Semi-variogram analysis

Geostatistical parameters		Variables			
		Al_2O_3	SiO_2	Fe_2O_3	TiO_2
Semi-variogram model		Spherical			
Nugget variance, C_o $(\%)^2$		15.75	2.33	31.00	0.153
Continuity variance, C $(\%)^2$		8.05	1.08	10.73	0.056
Range of influence, a (m)		170	220	260	170
Nugget to Sill Ratio (C_o: ($C+C_o$))		0.66	0.68	0.74	0.73
Zone of search (m)	Along easting (X)	170	170	170	170
	Along northing (Y)	170	170	170	170
	Along elevation (Z)	30	30	30	30
Min. no. of samples to krige a point		4	4	4	4
Max. no. of samples to krige a point		16	16	16	16
Number of points available for kriging		1017	1017	1017	1017
No. of points kriged		1017	1017	1017	1017
Mean of points used for kriging, Z (%)		41.78	2.81	27.28	2.07
Mean of kriged estimates, Z* (%)		41.79	2.77	27.30	2.07
Variance of points used for kriging $(\%)^2$		23.97	3.43	41.73	0.21
Mean kriging variance, KV $(\%)^2$		18.05	2.62	35.69	0.17
Mean estimated variance, EV $(\%)^2$		18.80	2.48	36.21	0.17
Ratio of EV: KV		1.04	0.95	1.01	1.00
Mean difference of true value from estimated values, Z- Z* (%)		-0.01	0.04	-0.02	0.00
Absolute mean difference | (Z- Z*) | (%)		3.403	1.24	4.74	0.314

Block Kriging

A selective mining unit or block size of 25m×25m×4m has been considered for kriging in a 3D grid from south-west to north-east of the deposit on the basis of one quarter of average sample spacing (David, 1977) along lateral directions and the mining bench height in practice, in vertical direction. A total of 17 horizontal slices were generated with a bench height of 4m starting from top (1242 mRL) to bottom (1178 mRL) of the deposit. Mineralized boundaries were then delineated on each slice. The dimensions of block model depends on geological characteristics of the deposit and mine planning considerations (Rossi and Deutsch, 2014). On each of the slices, blocks completely falling within the mineralized boundaries including the peripheral blocks containing greater than or equal to 50% mineralization were considered as mineralized blocks. These blocks were then considered for block kriging along with necessary input parameters, viz. (i) a minimum of 4 samples (because of the necessity to define a surface) and a maximum of 16 samples (because of reasonable computational time) with at least one sample falling in each quadrant to krige a block since the neighbourhood analysis involved a quadrant search (Sinclair and Blackwell, 2004); and (ii) radius of search for sample points around a block centre to be within the semi-variogram range of influence of Al_2O_3.

3D block kriging employing ordinary kriging (OK) approach has been used for estimation of block values. Semi-variogram model parameters and a block matrix, consisting of coordinates (easting, northing and elevation) of the initial block, number of blocks along easting, northing and elevation, total number of blocks to be kriged per bench slice within the framework of the delineated mineralized boundaries, provided necessary inputs to the kriging procedure. The

Table 3. Summary results of block kriging

Parameters	Al_2O_3	SiO_2	Fe_2O_3	TiO_2
Total number of blocks	6033	6033	6033	6033
Number of blocks kriged	5974	5974	5974	5974
Minimum kriged estimate (%)	30.87	1.10	19.08	1.49
Maximum kriged estimate (%)	50.32	6.82	34.11	2.89
Mean kriged estimate (%)	42.04	2.88	27.27	2.08
Minimum kriging variance $(\%)^2$	2.24	0.25	3.29	0.01
Maximum kriging variance $(\%)^2$	13.90	2.31	20.03	0.08
Mean kriging variance $(\%)^2$	5.27	0.56	6.88	0.03

procedure adopted includes selection of samples lying within the radius of search, establishment of kriging matrices along with setting of a semi-variance matrix with expected variability between each of the closest surrounding sample values and themselves, establishment of kriging matrices. Calculation of weight coefficients, multiplication of weight coefficients by their corresponding sample values have been performed to arrive at kriged estimates while the kriging variance has been calculated from the sum of the products of the weight coefficients and their corresponding sample to block variances. The procedure provided spatial distribution of kriged blocks within the limits of mineralized boundaries (Pandey et al., 2005). A summary results of block kriging in terms of total number of blocks kriged, minimum value, maximum value, mean kriged estimate and mean kriging variance are given in Table 3. Spatial distribution maps of kriged estimate and kriging variance in respect of Al_2O_3 and SiO_2 for one such representative bench slice at 1182 mRL are displayed in Fig. 6. While the spatial distribution map of kriged estimate provide the lateral display of the block estimates and its variation, the spatial distribution map of kriging variance reflect zones of uncertainty of varying magnitude associated with block estimates. The resulting kriged estimated block Al_2O_3 grades vary spatially between 30.87% and 50.32% with kriging variance ranging between 2.24$(\%)^2$ and 13.90$(\%)^2$, while SiO_2 grades vary spatially between 1.10% and 6.82% with kriging variance ranging between 0.25$(\%)^2$ and 2.31$(\%)^2$ from south to north and west to east part of the study area. Higher values of Al_2O_3 occur in patches and decrease outward. Kriging variance, being a function of characteristics of mineralisation as represented by semi-variogam, size and shape of a block being estimated total number of samples used to estimate a block, and relative position of samples with respect to each other as well as with respect to the block being estimated, defines the magnitude of uncertainty associated with the kriged estimate of a block. In this case, the magnitude of kriging variance is high at places indicating either inadequate number of samples around the block being estimated or decayed interrelationship among the samples and blocks estimated. The central part of the deposit is apparently a patch with high clay where no drilling has been carried out by the agency concerned. It is suggested that blast-hole sampling from the high kriging variance block/bench area would provide an improved grade control plan and blending schedule. The multiple colour code kriging grade and variance mapping (Fig. 6) would be of immense importance, most suitable, with an adequate understanding and applications at executional, operational and management execution levels.

Mineral Inventory

A 3-D representation of blocks with kriged estimates and kriging variances in respect of individual slices stacked one below the other from top to bottom provided the total volume of ground containing bauxite. Such a stacking representation of the blocks led to development of a mineral inventory for the deposit. In all, 17 slices with a total of 5974 blocks with dimensions as 25m x 25m× 4m were kriged. An average bulk density of 2 t/m^3 was considered for estimation of bauxite tonnage. This provided an estimated bauxite inventory of

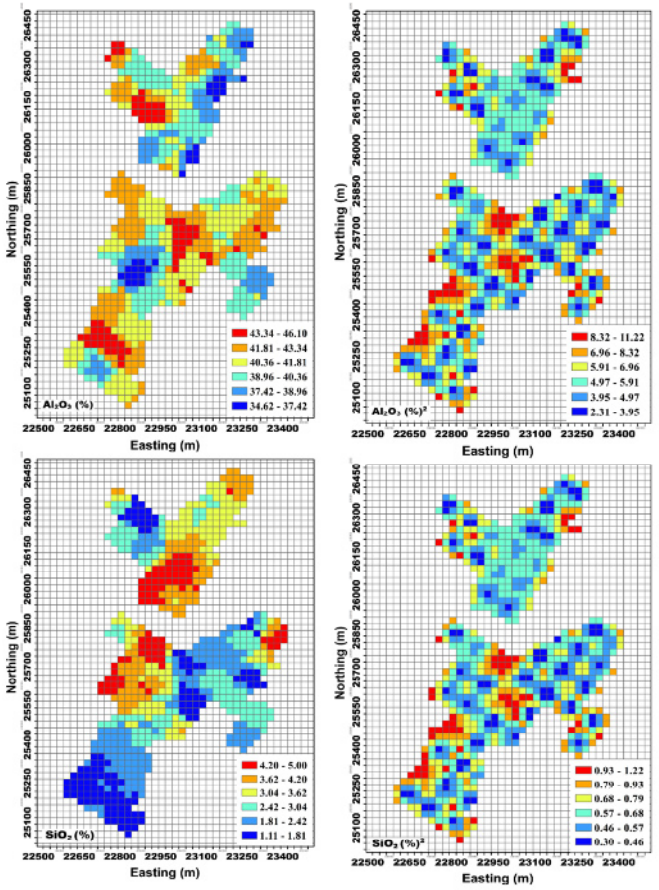

Fig.6. Spatial distribution maps of block kriged estimate (left) and kriging variance (right) in respect of Al_2O_3 and SiO_2 of a representative slice at 1182 mRL

Table 4. Mineral inventory of northern part of the bauxite deposit

Slice (mRL)	No. of blocks kriged	Vol. of bauxite (m^3)	Tonnage of bauxite (t)	Al_2O_3		SiO_2	
				KE (%)	KV (%)	KE (%)	KV (%)
1242	154	385000	770000	42.88	5.21	3.86	0.54
1238	238	595000	1190000	42.56	5.03	3.50	0.53
1234	297	742500	1485000	42.20	5.13	3.44	0.54
1230	360	900000	1800000	42.63	5.10	3.42	0.54
1226	339	847500	1695000	42.81	5.15	3.31	0.54
1222	248	620000	1240000	43.31	5.22	3.01	0.55
1218	246	615000	1230000	43.84	5.40	2.98	0.56
1214	241	602500	1205000	43.88	5.43	2.93	0.56
1210	250	625000	1250000	43.32	5.36	2.65	0.54
1206	296	740000	1480000	42.52	5.24	2.56	0.55
1202	299	747500	1495000	42.10	5.26	2.46	0.56
1198	374	935000	1870000	41.73	5.20	2.47	0.55
1194	376	940000	1880000	41.68	5.33	2.37	0.56
1190	482	1205000	2410000	41.44	5.55	2.36	0.58
1186	467	1167500	2335000	41.21	5.26	2.62	0.57
1182	702	1755000	3510000	40.77	5.33	2.91	0.58
1178	605	1512500	3025000	40.97	5.41	3.05	0.60

Total number of blocks kriged = 5974;
Bauxite volume of each block = 25m × 25m× 4m;
Total volume of bauxite = 14,935,000 m^3;
Average bulk density = 2 t/m^3 ;
Total tonnes of bauxite = 29.87 mt
Mean kriged estimate (KE) of Al_2O_3 = 42.04 %
Mean kriging variance (KV) of Al_2O_3 = 5.27 $(\%)^2$
Mean kriged estimate (KE) of SiO_2 = 2.88 %
Mean kriging variance (KV) of SiO_2 = 0.56 $(\%)^2$

Table 5 Grade-tonnage relations of Al_2O_3

Grades (C.I)	No. of blocks (f)	Class Av. (A)	E = (f/n)	CE	E×A	C(E×A)	C/O (%)	Avg. Al_2O_3	r_0 (mt)	W/O ratio
30-32	3	31	0.001	1.000	0.01	42.04	30	42.04	29.87	0.00
32-34	8	33	0.001	0.999	0.04	42.02	32	42.46	29.85	6.70×10^{-4}
34-36	9	35	0.002	0.998	0.05	41.98	34	42.40	29.81	2.01×10^{-3}
36-38	115	37	0.019	0.997	0.71	41.92	36	42.34	29.77	3.36×10^{-3}
38-40	926	39	0.155	0.977	6.04	41.21	38	42.48	29.19	0.02
40-42	1933	41	0.324	0.822	13.26	35.17	40	42.89	24.56	0.22
42-44	1971	43	0.330	0.499	14.18	21.90	42	44.69	14.90	1.00
44-46	641	45	0.107	0.169	4.82	7.71	44	48.18	5.04	4.93
46-48	245	47	0.041	0.062	1.92	2.88	46	49.00	1.84	15.23
48-50	114	49	0.019	0.021	0.93	0.96	48	49.50	0.61	47.97
50-52	9	51	0.002	0.002	0.07	0.02	50	50.66	0.04	745.75

CE = Cumulative expectancy; C(E×A) = Cumulative product of expectancy (E) and Class Av. (A); C/O: Cutoff grade of Al_2O_3; t_o: total tonnes of bauxite; Av. Al_2O_3 above cutoff = C(E×A) / CE; $r_{o:}$ tonnes of bauxite above cutoff = t_o x CE; W/O ratio = $(t_o-r_o)/r_o$.

Table 6. Grade-tonnage relations of SiO_2

Grades (C.I)	No. of blocks (f)	Class Av. (A)	E = (f/n)	CE	E×A	C(E×A)	C/O (%)	Avg. SiO	r_0 (mt)	W/O ratio
1.00-1.57	381	1.28	0.064	1.000	0.08	2.87	1.00	2.88	29.88	0.00
1.57-2.14	1134	1.85	0.190	0.936	0.35	2.79	1.57	2.98	27.98	0.07
2.14-2.71	1438	2.42	0.241	0.746	0.58	2.44	2.14	3.27	22.31	0.34
2.71-3.28	1187	2.99	0.199	0.506	0.59	1.86	2.71	3.67	15.12	0.98
3.28-3.85	899	3.56	0.150	0.307	0.54	1.26	3.28	4.10	9.18	2.25
3.85-4.42	585	4.13	0.098	0.157	0.40	0.73	3.85	4.63	4.69	5.37
4.42-4.99	197	4.70	0.033	0.059	0.15	0.32	4.42	5.45	1.76	15.98
4.99-5.56	26	5.27	0.004	0.026	0.02	0.17	4.99	6.41	0.78	37.31
5.56-6.13	48	5.84	0.008	0.022	0.05	0.14	5.56	6.64	0.65	44.97
6.13-6.70	19	6.41	0.003	0.014	0.02	0.10	6.13	7.12	0.41	71.88
6.70-7.27	62	6.98	0.010	0.010	0.07	0.08	6.70	7.34	0.31	95.39

CE = Cumulative Expectancy; C(E×A) = Cumulative product of expectancy (E) and Class Av. (A); C/O: Cutoff grade of SiO_2; t_o: total tonnes of bauxite; Av. SiO_2 above cutoff = C(E×A) / CE; $r_{o:}$ tonnes of bauxite above cutoff = t_o x CE; W/O ratio = $(t_o-r_o)/r_o$.

29.87 mt with mean kriged estimate as 42.04% Al_2O_3 and 2.88% SiO_2 with mean kriging variance as 5.27 $(\%)^2$ and 0.56 $(\%)^2$ respectively. Estimated mineral inventory of the deposit is provided in Table 4.

Grade-Tonnage Relationship

Grade-tonnage relationship constitutes an important interpretation of the summarized results of mineral inventory (Sarkar et al., 1988; Sinclair and Blackwell, 2004; Pandey et al., 2005, Sarkar, 2005) that aids in follow-up decisions for mine planning and design. It is a vital analysis for estimation of tonnages and grades available at various probabilistic cutoff grades. As the cutoff grade has a phenomenal impact on mineral inventory, a series of grade-tonnage relationships at various cutoff grades have been estimated. Grade-tonnage relationships have been established with respect to alumina and silica since these two in combination decide cutoff grade criteria for aluminium industry. Usually, tonnage at a lower cutoff grade is high and it progressively decreases with increasing cutoff grade (Sarkar, 2014(a) and (b); Gandhi and Sarkar, 2016). The relationships have been derived employing a simple numerical approach involving a step-wise integration of the block grade frequency curve over a range of kriged estimated block grades that calculates (i) quantities of ore and waste; (ii) average grade of ore and waste; (iii) waste-to-ore ratio at various probabilistic cutoff grades. Plots of these relationship provided grade-tonnage curves, both for Al_2O_3 and SiO_2. The grade-tonnage relationships derived are given in Table 5 for Al_2O_3 and in Table 6 for SiO_2 and the grade-tonnage curves are displayed in Fig.7. Tonnage vs. grade estimation provides economical options by which maximum profit could be established and thereby used as an aid to economic decisions for mineral industry. The geostatistically derived grade-tonnage relationships is a vital tool for effecting mine decisions.

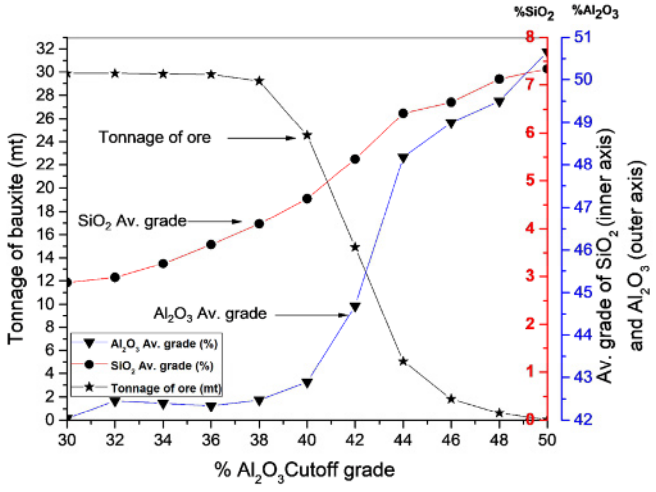

Fig.7. Grade-tonnage curves in respect of Al_2O_3 and SiO_2

CONCLUSIONS

The bauxite deposit studied is a high iron type (ferruginous) deposit and is statistically characterized as negatively skewed lognormal in terms of Al_2O_3 and Fe_2O_3 distributions and as positively skewed lognormal in terms of SiO_2 and TiO_2 distributions. The deposit is associated with moderate to high nugget-to-sill ratio and a moderate range of influence, reflecting geostatistical characteristics of

ferruginous bauxite deposit formed due to the weathering and residual enrichment through differential leaching. The integrated geostatistical modelling of the bauxite deposit combines deposit geology with statistical and geostatistical parameters and provides a cogent deposit appraisal. The approach delivers an objective means to geostatistical characterization, delineation of mineralized boundaries, mineral inventory estimation with assessment of associated uncertainty, and establishment of grade-tonnage relationships.

Acknowledgements: The authors are thankful to various exploration and mining agencies for necessary data support and to the host institution and the department for providing infrastructure facilities.

References

Babu, P.S., Majumdar T.J., Bhattacharya, A.K. (2014) Study of spectral signatures for exploration of Bauxite ore deposits in Panchpatmali, India. Geocarto Internat., v.30 (5), pp.37–41.

Bhukte, P.G. and Chaddha, M.J. (2014) Geotechnical evaluation of Eastern Ghat Bauxite Deposits of India. Jour. Geol. Soc. India, v.84(2), pp.227-238.

David, M. (1977) Geostatistical Ore Reserve Estimation. Elsevier Scientific Publ., Amsterdam, Netherlands, 364p.

Diko, L., Vervoort A. and Vergauwen, I. (2001) Geostatistical modelling of lateritic bauxite orebodies in Surinam: Effect of the vertical dimension. Jour. Geochem. Explor., v.73 (3), pp.131–153.

Gandhi, S.M. and Sarkar, B.C. (2016) Essentials of Mineral Exploration and Evaluation. Elsevier, Amsterdam, Netherlands, 406p.

Olea, R.A. (1999) Geostatistics for Engineers and Earth Scientists. Kluwer Academic Publishers; Boston, 303p.

Pandey, S., Saikia, K., Sarkar, B.C. (2005) Geostatistical modelling in presence of trend – a test case of a bauxite deposit in Jharkhand, India. Applied Earth Sci., v.114 (1), pp.1–13.

Pyrcz, M.J. and Deutsch, C.V. (2006) Semi-variogram models based on geometric offsets. Mathematical Geol., v.38 (4), pp.475-488.

Ramakrishnan, M. and Vaidyanadhan, R. (2010) Geology of India. Geological Society of India, Bangalore, v.1, pp.335-365.

Rossi, M.E. and Deutsch, C.V. (2014) Mineral Resource Estimation. Springer, Dordrecht, 332p.

Saikia, K. and Sarkar, B.C. (2013) Coal exploration modelling using geostatistics in Jharia coal field, India. Internat. Jour. Coal Geol., v.112 , pp.36–52.

Sarkar, B.C. (2005) Developments in geomathematical modelling and computer applications in mineral resources assessment. Jour. Geol. Soc. India, v.66(6), pp.713-724.

Sarkar, B.C. (2014a) Geostatistics: Concepts and Applications in Mineral Deposit Modelling for Exploration and Mining. Jour. Indian Geol. Congress, v.6 (1), pp.3-16.

Sarkar, B.C. (2014b) Geostatistics for Natural Resources Modelling. Proc. Brain Storming Workshop on Geostatistics, BSWG 2014, Dept. of Applied Geology, ISM Dhanbad.

Sarkar, B.C., O'Leary, J., Mill, A.J.B. (1988) An integrated approach to geostatistical evaluation. Mining Magz., v.159(3), pp.199–207.

Sen, A.K. and Guha, S. (1987) The geochemistry of the weathering sequences-present and past - in and around the Pottangi and Panchpatmali Bauxite-Bearing Plateaus. Chemical Geol., v.63, pp.233–274.

Sengupta, D.K., Som, S.K., Misra, U. (1991) Lineaments and tectonic analysis through landsat imagery and its implications on the evaluation of bauxite and laterite deposits in and around Panchpatmali area, Koraput district, Orissa. Jour. Indian Soc. Remote Sensing, v.19(3), pp.187-194.

Sinclair, A.J. and Blackwell, G.H. (2004) Applied Mineral Inventory Estimation. Cambridge Univ. Press, Cambridge, 381p.

Sharma, R.S. (2009) Cratons and fold belts of India. Springer Publ. pp. 231-257.

Subrahmanyam, A.V., Rao, M.J., Rao, J.S.R.K. (1996) Nodular laterite from Panchpatmali bauxite deposit, Koraput dist, Orissa, evidence for neotectonism from east coast bauxite province. Indian Jour. Earth Sci., v.23(2-3), pp.147-160.

Wellmer, F.W. (1998) Statistical evaluations in exploration for mineral deposits. Springer Publ., 379p.

(Received: 29 December 2018; Revised form accepted: 7 February 2019)